Journal of Medicinal Chemistry Article

J. Med. Chem. **2010,** *53,* 4119–4129 **4119**
DOI: 10.1021/jm100143f

Sequence Inversion and Phenylalanine Surrogates at the β-Turn Enhance the Antibiotic Activity of Gramicidin S

Concepción Solanas,[†] Beatriz G. de la Torre,[‡] María Fernández-Reyes,[§] Clara M. Santiveri,[∥] M. Ángeles Jiménez,[∥] Luis Rivas,[§] Ana I. Jiménez,[†] David Andreu,*[,‡] and Carlos Cativiela*[,†]

[†]*Departamento de Química Orgánica, Instituto de Ciencia de Materiales de Aragón, Universidad de Zaragoza−CSIC, Pedro Cerbuna 12, 50009 Zaragoza, Spain,* [‡]*Departament de Ciències Experimentals i de la Salut, Universitat Pompeu Fabra, Dr. Aiguader 88, 08003 Barcelona, Spain,* [§]*Centro de Investigaciones Biológicas, CSIC, Ramiro de Maeztu 9, 28040 Madrid, Spain, and* [∥]*Instituto de Química-Física Rocasolano, CSIC, Serrano 119, 28006 Madrid, Spain*

Received February 3, 2010

A series of gramicidin S (GS) analogues have been synthesized where the Phe ($i + 1$) and Pro ($i + 2$) residues of the β-turn have been swapped while the respective chiralities (D-, L-) at each position are preserved, and Phe is replaced by surrogates with aromatic side chains of diverse size, orientation, and flexibility. Although most analogues preserve the β-sheet structure, as assessed by NMR, their antibiotic activities turn out to be highly dependent on the bulkiness and spatial arrangement of the aromatic side chain. Significant increases in microbicidal potency against both Gram-positive and Gram-negative pathogens are observed for several analogues, resulting in improved therapeutic profiles. Data indicate that seemingly minor replacements at the GS β-turn can have significant impact on antibiotic activity, highlighting this region as a hot spot for modulating GS plasticity and activity.

Introduction

Increasing resistance of bacteria to conventional antibiotics has posed a serious threat to human health and generated a growing need for new drugs to combat microbial infection. Cationic antimicrobial peptides (AMPs[a]) from either microbial or eukaryotic sources have been proposed as an alternative to conventional antibiotics because their lethal mechanism, based on disruption of the pathogen's cytoplasmic membrane, differs from those of most conventional antibiotics in clinical use and makes induction of resistance rather unlikely.[1,2]

Gramicidin S (GS), one of the best-studied cationic AMPs, is synthesized nonribosomally by *Bacillus brevis*[3] and active against bacteria and fungi.[4,5] GS is a cyclic symmetrical decapeptide, *cyclo*(Val-Orn-Leu-D-Phe-Pro)$_2$ (Figure 1), that adopts a pleated β-sheet structure[6−8] in which the Val, Orn, and Leu residues align to form two antiparallel β-strands. Two type-II′ β-turns centered at the D-Phe-Pro sequences flank the β-strands, stabilized by four cross-strand hydrogen bonds (Figure 1). Amphipaticity of the β-sheet structure is achieved by positioning of the hydrophobic side chains of Leu and Val facing one side of the molecule, whereas the two basic Orn residues project to the opposite side.[5,9]

Although the mechanism of action of GS is not completely understood,[10] it is generally accepted that the peptide kills bacterial cells through destabilization and permeabilization of their cytoplasmic membranes.[11] Unfortunately, GS displays poor selectivity between microbial and mammalian cells, a fact that restricts its use to topical applications.[5] In recent years, considerable effort has been devoted to developing GS analogues with improved therapeutical index where the antimicrobial and cytotoxic (e.g., hemolytic) activities are dissociated. In this quest, both the β-strand[12−14] and the β-turn[15−25] regions have been extensively modified in SAR studies that have shed light on factors governing GS bioactivity such as cationic nature,[11,24] amphipathic character,[26,27] β-sheet structure,[24,26,27] ring size,[28] and global hydrophobicity.[26,27] The latter property results not only from the hydrophobic domain defined by the Val and Leu side chains at the β-strands but also from the presence of an aromatic side chain at the two β-turn regions that is regarded as essential for bioactivity.[15−17,24,29−32] Indeed, replacement of D-Phe by either Gly, D-Ala, or D-cyclohexylalanine leads to less active or inactive compounds,[29,30] thus evidencing that an aromatic group at this particular position is needed for full

*To whom correspondence should be addressed. For D.A.: phone, +34-933160868; fax, +34-933160901; e-mail, david.andreu@upf.edu. For C.C.: phone, +34-976761210; fax, +34-976761210; e-mail, cativiela@unizar.es.

[a]Abbreviations: Ac$_3$c, 1-aminocyclopropanecarboxylic acid; AMP, antimicrobial peptide; ATCC, American Type Culture Collection; (αMe)Phe, α-methylphenylalanine; Boc, *tert*-butoxycarbonyl; CECT, Spanish Type Culture Collection; COSY, correlated spectroscopy; c$_3$diPhe, 1-amino-*c*-2,*t*-3-diphenylcyclopropane-*r*-1-carboxylic acid; c$_3$Phe, 1-amino-2-phenylcyclopropanecarboxylic acid; Dbg, dibenzylglycine; DIEA, *N*,*N*-diisopropylethylamine; Dip, β,β-diphenylalanine; DMF, *N*,*N*-dimethylformamide; DSS, sodium 2,2-dimethyl-2-silapentane-5-sulfonate; ESI, electrospray ionization; Flg, fluorenylglycine; For, formyl; GS, gramicidin S; HATU, 2-(7-aza-1*H*-benzotriazole-1-yl)-1,1,3,3-tetramethyluronium hexafluorophosphate; HBTU, 2-(1*H*-benzotriazole-1-yl)-1,1,3,3-tetramethyluronium hexafluorophosphate; HC$_{50}$, 50% hemolytic concentration; HOAt, *N*-7-azahydroxybenzotriazole; HRMS, high resolution mass spectrometry; HSQC, heteronuclear single quantum coherence spectra; LPS, lipopolysaccharide; MIC$_{50}$, minimal inhibitory concentration; NOESY, nuclear Overhauser enhancement spectroscopy; Orn, ornithine; rmsd, root-mean-square deviation; SAR, structure−activity relationship; TFA, trifluoroacetic acid; TFMSA, trifluoromethanesulfonic acid; TI, therapeutic index (HC$_{50}$/MIC$_{50}$); Tic, 1,2,3,4-tetrahydroisoquinoline-3-carboxylic acid; TIS, triisopropylsilane; TOCSY, total correlated spectroscopy.

Published on Web 04/22/2010

bactericidal potency. Moreover, by replacing the D-Phe residues in GS by a variety of noncoded aromatic amino acids, we have recently shown[25] that the pharmacological profile changes dramatically with the size and spatial arrangement of the aromatic side chain at the $i + 1$ position of the β-turns.

These latter findings have led us to question whether an aromatic moiety is strictly necessary at the $i + 1$ position of the β-turn. In line with this, we hypothesized that the $i + 1$ and $i + 2$ positions could be swapped without dramatic alteration of GS overall architecture (i.e., the β-turns and the whole β-sheet structure) as long as the chirality of the said $i + 1$ and $i + 2$ positions (D- and L-, respectively) remained unaltered, as in peptide **1** (Figure 1). The hypothesis is supported on the known requirement for a D-amino acid (or glycine) at the $i + 1$ position[33] of type II′ β-turns such as that in GS and on the fact that Pro is the amino acid residue with the highest propensity to occupy an $i + 1$ position at a type-II β -turn;[33−35] therefore, a D-Pro at the $i + 1$ position would appear to be an optimal choice for nucleating a type II′ β-turn. Herein we report on a family of GS analogues bearing double modifications based on the aforementioned considerations. Specifically, in the lead analogue **1**, *cyclo*(Val-Orn-Leu-D-Pro-Phe)$_2$ (Figure 1), both D-Phe-Pro sequences in GS have been replaced by D-Pro-Phe. In the remaining analogues of the series, Phe is replaced by a variety of nonproteinogenic counterparts bearing aromatic side chains of different size, orientation, and flexibility. The structure of these GS analogues has been analyzed by NMR spectroscopy and related to their antibiotic and hemolytic activities.

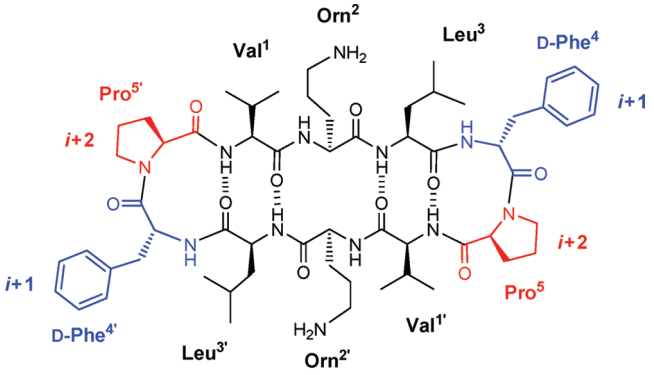

cyclo(Val-Orn-Leu-**D-Phe-Pro**)$_2$ (GS)

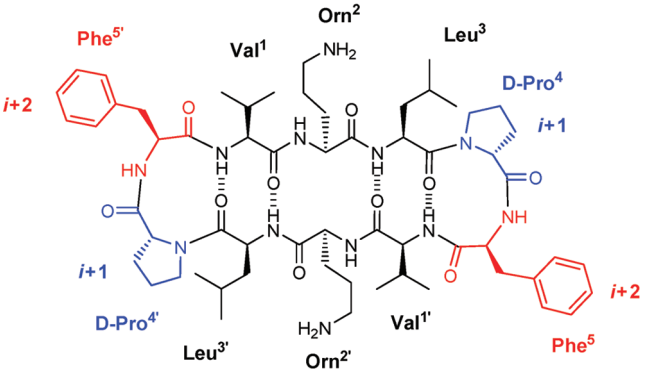

cyclo(Val-Orn-Leu-**D-Pro-Phe**)$_2$ (**1**)

Figure 1. Structure of gramicidin S (top) and the analogue generated (**1**) by sequence inversion at the β-turn (bottom). In both cases, the peptide adopts a β-sheet structure.

Results

Peptide Design and Synthesis. The amino acids selected as Phe replacements (Phe*) in the GS analogue **1** (Figure 1) are shown in Figure 2. β,β-Diphenylalanine (Dip), fluorenylglycine (Flg), dibenzylglycine (Dbg), 1,2,3,4-tetrahydroisoquinoline-3-carboxylic acid (Tic), and the two enantiomers of the cyclopropane amino acid $c_3$diPhe were initially considered. Most of them incorporate two phenyl rings exhibiting diverse orientations and degrees of conformational freedom. In Dbg, the aromatic substituents can freely rotate, whereas in $c_3$diPhe they are tightly held. Both Dip and Flg bear two phenyl groups on the same β carbon that in the latter case are forced to be coplanar. The orientation of the aromatic moiety in Tic is fixed by the methylene unit linking it to the backbone. In addition, it should be noted that Dbg is achiral while $c_3$diPhe is characterized by an achiral α carbon and two chiral β carbons. To evaluate separately the structural effect associated exclusively to the strained three-membered cycle

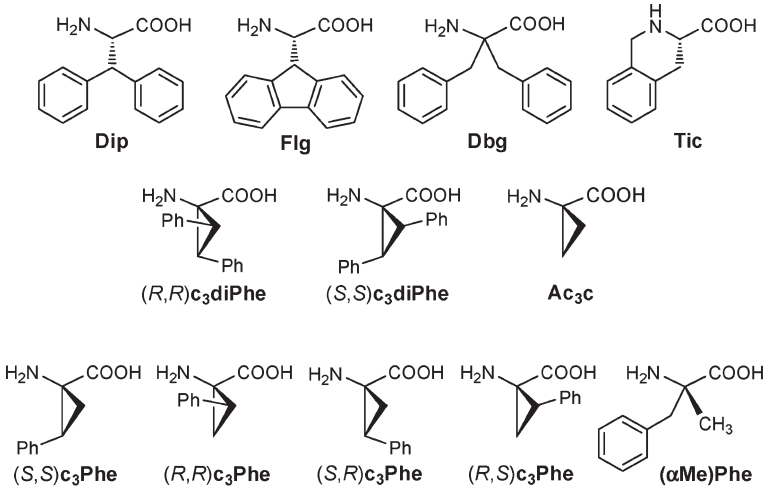

2 *cyclo*[Val-Orn-Leu-D-Pro-**Dip**]$_2$
3 *cyclo*[Val-Orn-Leu-D-Pro-**Flg**]$_2$
4 *cyclo*[Val-Orn-Leu-D-Pro-**Dbg**]$_2$
5 *cyclo*[Val-Orn-Leu-D-Pro-**Tic**]$_2$
6 *cyclo*[Val-Orn-Leu-D-Pro-(*R*,*R*)**c$_3$diPhe**]$_2$
7 *cyclo*[Val-Orn-Leu-D-Pro-(*S*,*S*)**c$_3$diPhe**]$_2$
8 *cyclo*[Val-Orn-Leu-D-Pro-**Ac$_3$c**]$_2$

9 *cyclo*[Val-Orn-Leu-D-Pro-(*S*,*S*)**c$_3$Phe**]$_2$
10 *cyclo*[Val-Orn-Leu-D-Pro-(*R*,*R*)**c$_3$Phe**]$_2$
11 *cyclo*[Val-Orn-Leu-D-Pro-(*S*,*R*)**c$_3$Phe**]$_2$
12 *cyclo*[Val-Orn-Leu-D-Pro-(*R*,*S*)**c$_3$Phe**]$_2$
13 *cyclo*[Val-Orn-Leu-D-Pro-**(αMe)Phe**]$_2$

Figure 2. Amino acids selected as L-Phe replacements (Phe*) in **1** (left). Sequence and numbering of the corresponding gramicidin S analogues generated (**2**−**13**) (right). For amino acids containing two chiral centers, configurations are given for the 2,3 (in $c_3$diPhe) or 1,2 (in c_3Phe) carbon atoms.

Scheme 1. Synthetic Strategy for the GS Analogues[a]

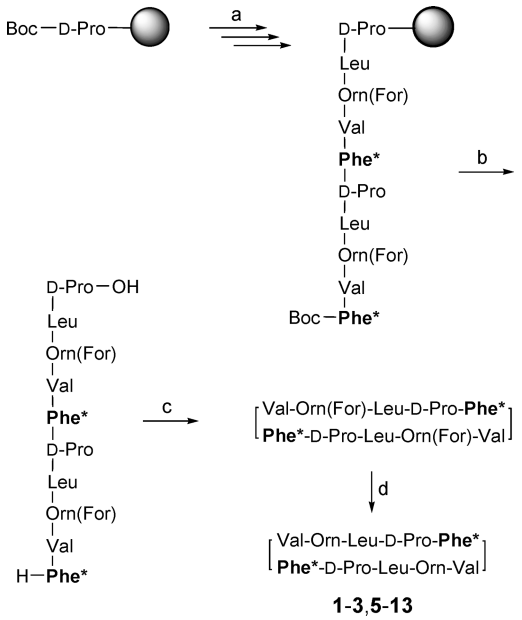

[a] Reagents and conditions: (a) standard solid-phase peptide synthesis (Boc chemistry); (b) TFA/TFMSA/TIS 10:1:1, rt, 90 min; (c) HATU/HOAt/DIEA (3:3:5 equiv), DMF, rt, 1 h; (d) 20% HCl in MeOH, 37 °C, 21 h. Phe* stands for Phe or the corresponding substitute.

present in $c_3$diPhe, the unsubstituted cyclopropane amino acid Ac_3c was also considered for this study. Cyclopropane amino acids have been shown to exert a strong stabilizing effect on β-turns when incorporated into Pro-Xaa dipeptides[36] and are therefore expected to stabilize the β-sheet structure of GS, provided no steric conflict between the cyclopropane substituents and the contiguous residues arises.

The different antibiotic properties found for the peptides incorporating the two $c_3$diPhe enantiomers (see below) prompted us to evaluate the effect produced by the cyclopropane amino acid bearing a single phenyl substituent, c_3Phe (Figure 2). In this case, four stereoisomeric forms are possible, each of them with a different orientation of the aromatic ring. It is worth noting that each $c_3$diPhe residue can be regarded as formally containing the aromatic side chain of two c_3Phe stereoisomers. Additionally, α-methylphenylalanine [(αMe)Phe] was included in this study as the open-chain counterpart of c_3Phe, in the same way as Dbg can be viewed as the acyclic equivalent of $c_3$diPhe. Both (αMe)Phe and Dbg keep the α-tetrasubstituted character of c_3Phe and $c_3$diPhe but not the restriction imposed by the three-membered ring. As an α-methylated amino acid, (αMe)Phe is also particularly suitable to occupy the $i + 2$ position of a β-turn.[37]

Solid-phase Boc chemistry protocols[19,23] were applied to the synthesis of peptides **1**−**13** (Figures 1,2), as done for GS and the first series of analogues in our previous work.[25] All stereoisomers of $c_3$diPhe, c_3Phe, and Flg shown in Figure 2 were obtained as *N*-Boc derivatives in enantiomerically pure form following previously reported procedures.[38−40] Achiral Boc-Dbg-OH was synthesized according to the protocol described by Kotha.[41] Boc-(αMe)Phe-OH was obtained from commercially available H-(αMe)Phe-OH, and the side chain of *N*-Boc ornithine was protected as a formamide as described by Kitagawa.[42] Each peptide was synthesized following the general route presented in Scheme 1. Unsuccessful coupling of the Dbg residue prevented the synthesis of the linear precursor of peptide **4**. For the remaining peptides, the solid-phase synthetic protocols were completed satisfactorily. The linear decapeptides were released from the polymeric support by treatment with TFMSA and then cyclized in solution under high-dilution conditions. Finally, deprotection of the Orn side chains by acid hydrolysis followed by reversed-phase HPLC purification furnished the target peptides (**1**−**3**, **5**−**13**) in good overall yields and high purity (≥99%, see Supporting Information). All peptides were satisfactorily characterized by MS and NMR.

NMR Structural Studies. The structure of GS analogues **1**−**3** and **5**−**13** was evaluated in aqueous solution by NMR as previously done for GS and a first series of analogues.[25] A set of minor NMR signals coexisting with those of the major species were present in the spectra of all analogues, except for peptide **5** (Figure 3, see also Supporting Information, Figure SF2, and Table ST1). In all cases, the major conformer was found to contain both Leu-D-Pro bonds in a *trans* arrangement, as inferred from the presence of an NOE between the Leu H_α proton and the Pro $H_{\delta\delta'}$ protons (Figure 3 and Table ST2, Supporting Information), as well as from the $^{13}C_\beta$−$^{13}C_\gamma$ chemical shift differences in the 2.9−5.2 ppm range observed for the Pro residues ($\Delta\delta^{Pro} = \delta^{C\beta} - \delta^{C\gamma}$ ppm; see Supporting Information, Table ST2).[44] For peptides **1**−**3**, as expected for Pro-containing peptides, the minor species were assigned to the *cis* rotamer of at least one Leu-D-Pro bond, as deduced from the presence of an NOE between the H_α protons of Leu and Pro residues and from a $\Delta\delta^{Pro}$ value near 10 ppm.[44] The most populated of the two minor species is an aymmetric conformer in which one Leu-D-Pro bond corresponds to the *trans* rotamer and the other to the *cis* rotamer, and the least populated is a symmetric conformer with the two Leu-D-Pro bonds in *cis* (Figure 3A, and Supporting Information, Table ST3). In contrast, analogues **6**−**13** showed broad NMR signals and, except for peptides **11** and **13**, exchange cross-peaks between signals belonging to the major and minor species, as well as between signals of different minor species, were observed in the 150 ms NOESY spectra (Supporting Information, Figure SF2 and Table ST1). This indicates that the conformational equilibrium in peptides **6**−**13** is faster than that usually associated to the isomerization of the Leu-D-Pro bonds. More strikingly, the minor species observed in peptides **6**, **7**, and **9** could not be attributed to the *cis*−*trans* isomerism of the amide bonds preceding Pro residues, as they exhibit NOEs between the Leu H_α proton and the Pro H_δ and $H_{\delta'}$ protons, and $\Delta\delta^{Pro}$ values below 5.0 ppm (Supporting Information, Figure SF2 and Table ST4), both typical of *trans* rotamers. Hence, the minor species observed for peptides **6**−**13** could not be attributed to the *cis*−*trans* isomerism of the amide bonds preceding Pro. Because these compounds (**6**−**13**) incorporate an α-tetrasubstituted amino acid, the observed conformational equilibrium could be somehow related to the presence of such nonproteinogenic residues. It should be noted that peptides **6**, **7**, and **9**−**13** contain Phe surrogates that are not only α-tetrasubstituted but also bear one (or more) bulky, rigidly held phenyl group(s) that could further hamper rotation about the bonds in the neighborhood of the α carbon. The presence of minor species, broad signals, and exchange NOE cross-peaks made the spectral analysis of some of these peptides rather complex (see Supporting Information, Tables ST2 and ST4). Results

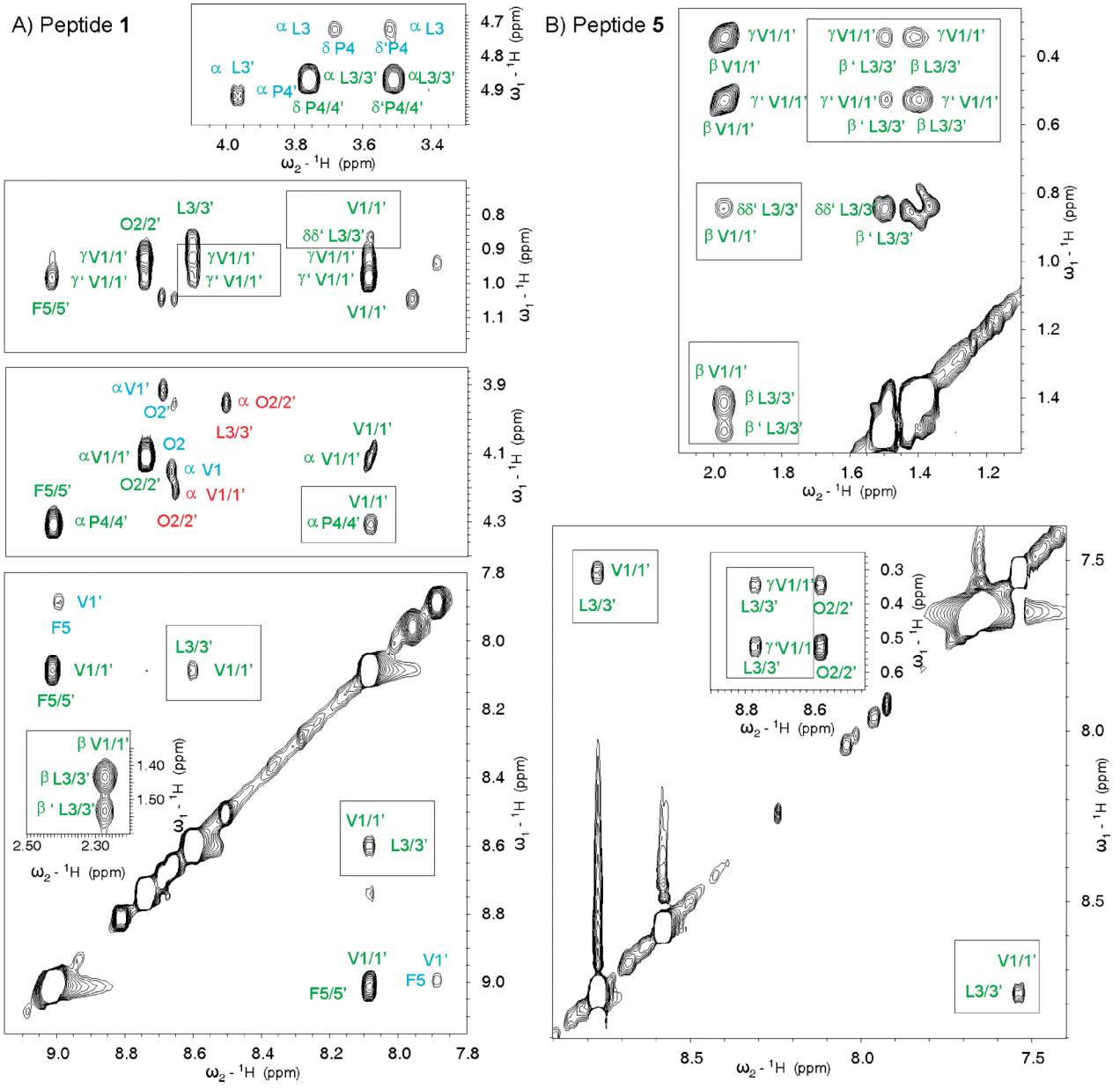

Figure 3. Selected NOESY spectral regions for peptides **1** (A) and **5** (B) in D_2O (top panels) and in H_2O/D_2O 9:1 v/v (all other panels) at pH 3 and 5 °C. Green, blue, and red labels correspond, respectively, to symmetrical major, asymmetrical minor, and symmetrical minor species. The top panel for peptide **1** shows the sequential NOEs between the Leu H_α proton and the Pro H_δ and $H_{\delta'}$ protons, indicative of the *trans* rotamery for the two Leu-Pro bonds in the major species, and for one Leu-Pro bond in the aymmetrical minor species, as well as the sequential NOE between the Leu and Pro H_α protons demonstrating the *cis* rotamery for one Leu-Pro bond in the aymmetrical minor species. Nonsequential NOEs, as those between the amide protons of Val1 and Leu3′, and Val1′ and Leu3 (Figure 1 and Table 2), are boxed.

described below correspond, in all cases, to the major *trans*−*trans* species.

Chemical shifts of $C_\alpha H$ protons and C_α carbons are dependent on the ϕ,ψ torsion angles and are, therefore, good indicators of the secondary structure adopted by the peptide backbone. Lys $\delta^{\text{random coil}}$ values[43] were used to calculate the $\Delta\delta$ values for the Orn residues. For all compounds investigated (Figure 4), Orn2/2′ and Leu3/3′ exhibited positive $\Delta\delta_{C\alpha H}$ conformational shifts ($\Delta\delta_{C\alpha H} = \delta_{C\alpha H}^{\text{observed}} - \delta_{C\alpha H}^{\text{random coil}}$, ppm) and negative $\Delta\delta_{C\alpha}$ values ($\Delta\delta_{C\alpha} = \delta_{C\alpha}^{\text{observed}} - \delta_{C\alpha}^{\text{random coil}}$, ppm), as expected for β-strand residues ($\Delta\delta_{C\alpha H} = +0.40$ ppm and $\Delta\delta_{C\alpha} = -1.6$ ppm on average in β-sheets).[45,46] The Orn2/2′ residues in **2** were the sole exception to this pattern. The $\Delta\delta_{C\alpha H}$ and $\Delta\delta_{C\alpha}$ profiles observed for Val1/1′ do not seem to follow a particular trend and adopt either positive or negative values. This anomalous behavior may be explained by the ring current effects generated by the aromatic groups in the contiguous position (Phe*5/5′), as observed in our previous work on GS analogues[25] and some β-hairpin peptides.[47] Indeed, in the absence of aromatic substituents (peptide **8**), Val1/1′ shows conformational shifts appropriate for a β-strand residue.

The large $^3J_{C\alpha H-NH}$ coupling constants observed for Val1/1′, Orn2/2′ and Leu3/3′ (8.0−9.8 Hz, Supporting Information, Table ST5) confirm that these residues adopt a β-sheet conformation. Again, in analogue **2**, the Orn2/2′ deviate from the expected behavior ($^3J_{C\alpha H-NH} = 5.7$ Hz). On the other hand, in the (*R*,*S*)c_3Phe derivative (**12**), the $^3J_{C\alpha H-NH}$ values of Val1/1′ and Leu3/3′ could not be determined because of signal broadening.

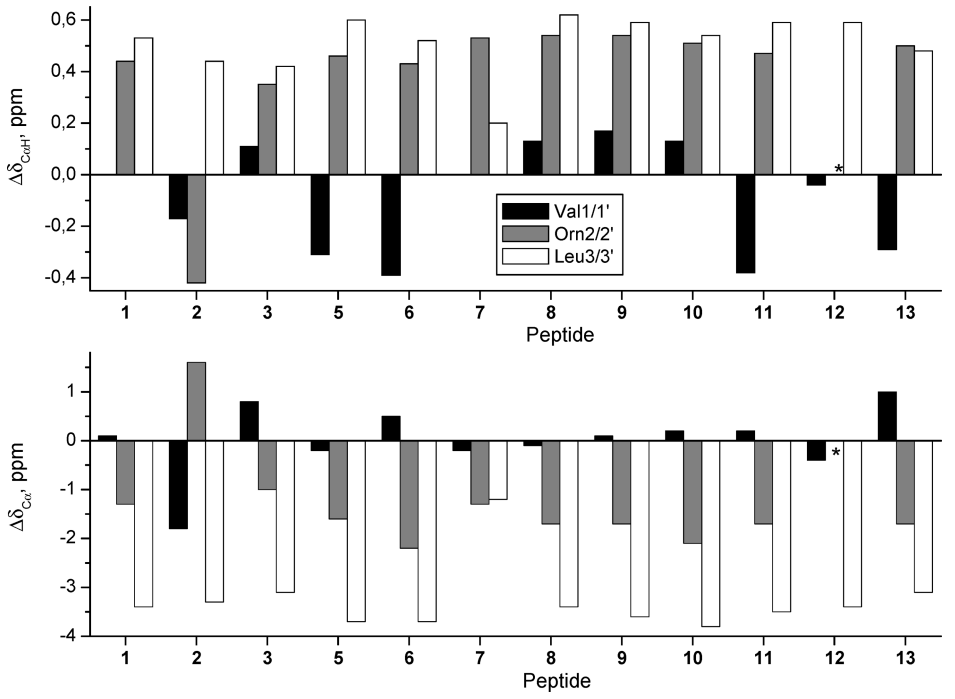

Figure 4. $\Delta\delta_{C\alpha H}$ and $\Delta\delta_{C\alpha}$ profiles ($\Delta\delta = \delta^{observed} - \delta^{random\ coil}$, ppm) for GS analogues in aqueous solution at pH 3.0 and 5 °C. Lys $\delta^{random\ coil}$ values[43] were used to calculate the $\Delta\delta$ values for the Orn residues. The $\delta_{C\alpha H}$ and $\delta_{C\alpha}$ values for the Orn residues in **12** could not be assigned.

Table 1. Temperature Coefficients[a] ($\Delta\delta/\Delta T$, ppb·K^{-1}) for the Amide Protons

peptide	Phe*[5,5'][b]	Val[1,1'] (NH)	Orn[2,2'] (NH)	Leu[3,3'] (NH)	Phe*[5,5'] (NH)
1	Phe	−2.2	−9.1	−1.8	−8.7
2	Dip	−2.9	−4.1	+0.9	−7.4
3	Flg	−0.7	−9.9	+2.6	−7.3
5	Tic	−2.0	−8.5	−3.8	—
6	(*R*,*R*)c$_3$diPhe	−3.2	−10.5	−4.2	−7.1
7	(*S*,*S*)c$_3$diPhe	−1.0	−9.0	−1.5	−9.0
8	Ac$_3$c	−1.9	−9.0	−5.1	−11.8
9	(*S*,*S*)c$_3$Phe	−1.6	−9.8	−4.0	Ov[c]
10	(*R*,*R*)c$_3$Phe	−2.1	−9.0	−3.9	−7.1
11	(*S*,*R*)c$_3$Phe	−3.1	−10.0	−3.7	−8.1
12	(*R*,*S*)c$_3$Phe	−7.5	−8.5	−10.0	−15.1
13	(αMe)Phe	−1.6	−7.0	−3.0	−9.9

[a] Measured in H_2O/D_2O 9:1 (v/v) at pH 3.0 and temperature range of 5−25 °C. [b] Phe* stands for Phe or the corresponding substitute. [c] Not determined because of signal overlapping.

The involvement of the NH amide protons in intramolecular hydrogen bonds was deduced from the temperature coefficients ($\Delta\delta/\Delta T$) (Table 1). The amide protons of Orn2/2′ and Phe*5/5′ displayed large negative $\Delta\delta/\Delta T$ values (below −7.0 ppb·K^{-1}) in all peptides, except again for analogue **2**, in agreement with their non-hydrogen bonded, solvent-exposed character in the GS β-sheet (Figure 1). In comparison, and with the exception of compound **12**, $\Delta\delta/\Delta T$ values above −5.1 ppb·K^{-1} were observed for the NH protons of Val1/1′ and Leu3/3′, which are involved in intramolecular hydrogen bonds in the GS structure (Figure 1).

The above structural data suggest that most analogues of this study fit into a β-sheet conformation, as does GS.[6−8,25] It is worth noting that, in almost all peptides of the series, the Val1/1′ NH exhibits the typical behavior of a hydrogen-bonded amide proton, which is not the case for either GS or the analogues in our previous work.[25] This may suggest that the peptides (with the probable exception of **2** and **12**) adopt a more regular β-sheet structure, which could be attributed to the presence of the D-Pro-Phe* instead of the D-Phe*-Pro sequence.

NOE data provided further structural information on the current set of analogues. The GS β-sheet structure (Figure 1) should give rise to five characteristic backbone proton NOEs: C_αH Orn2−C_αH Orn2′ (distance in a canonical antiparallel β-sheet: 2.2 Å), C_αH Orn2−NH Leu3′, C_αH Orn2′−NH Leu3 (distance in a canonical antiparallel β-sheet: 3.2 Å), NH Val1−NH Leu3′, and NH Val1′−NH Leu3 (distance in a canonical antiparallel β-sheet: 3.3 Å). Given the molecule symmetry, the first NOE would not be observable, the second and third ones will be undistinguishable from the sequential C_αH Orn2/2′−NH Leu3/3′ NOEs, while the last two must overlap into a single cross-peak. Such a cross-peak is indeed observed in the NOESY spectra of all peptides investigated (Table 2, Figure 3), with the exception of **2** and **12**, which once again deviate from the expected behavior. NOE data are also informative on the layout of the side chains. The backbone β-sheet conformation orients the Val and Leu side chains toward the same side of the molecule (Figure 1) and, indeed, NOE correlations between hydrogens of these side chains are observed for all peptides (Table 2, Figure 3) except **7**, for which spectrum complexity precluded analysis. The presence of such NOE cross-peaks in analogues **2** and **12** suggests that the Val and Leu side chains are proximal. This could translate into a certain amphiphilic character despite the fact that these GS analogues do not seem to adopt a canonical β-sheet structure.

Biological Activity. The **1**−**3** and **5**−**13** analogues (peptide **4** was not synthetically viable, see above) were tested along with GS against two Gram-positive (*Staphylococcus aureus* and *Listeria monocytogenes*) and two Gram-negative bacterial strains (*Acinetobacter baummanii* ATCC 19606 and an isogenic strain resistant to colistin (polymyxin E)). Although

Table 2. Summary of NOEs Observed[a]

		backbone NOE[d]	side-chain NOE[e]			
peptide[b]	Phe*[5,5′c]	NHVal[1]−NHLeu[3′]/NHVal[1′]−NHLeu[3]	Val[1,1′]−Leu[3,3′]	Orn[2,2′]−Phe*[5,5′]	Val[1,1′]−Phe*[5,5′]	D-Pro[4,4′]−Phe*[5,5′]
1	Phe	+	+	+	−	−
2	Dip	−	+	+	+	+
3	Flg	−[f]	+	−	+	+
5	Tic	+	+	−	+	−
6	(*R*,*R*)c$_3$diPhe	+	+	+[g]	+	+
8	Ac$_3$c	+	+	+[h]	−	+[h]
9	(*S*,*S*)c$_3$Phe	+	+	+[h]	+	+
10	(*R*,*R*)c$_3$Phe	+	+	+[h]	−	+
11	(*S*,*R*)c$_3$Phe	+	+	−	+	+[h]
12	(*R*,*S*)c$_3$Phe	−	+[h]	+	+	−
13	(αMe)Phe	+	+	+[h]	+	+

[a] Observation of one or more NOEs is shown by a "+", and nondetected NOEs by a "−". [b] Nonambiguous assignment of NOESY cross-peaks was precluded in peptide **7** because of its very broad signals and the presence of numerous exchange cross-peaks. [c] Phe* stands for Phe or the corresponding surrogate. [d] NOE involving backbone protons. [e] NOE involving at least one side chain proton of the residues indicated. [f] Not observed due to closeness to diagonal. [g] Weak peak intensities. [h] Only protons of the cyclopropane ring or the α-methyl group are involved.

Table 3. Hemolytic and Antimicrobial Activities[a] (μM) of Gramicidin S (GS) Analogues with Sequence Inversion at the β-Turn

		erythrocytes	*S. aureus*		*L. monocytogenes*		*A. baumanni S*		*A. baumannii R*[d]	
peptide	Phe*[5,5′b]	HC_{50}	MIC_{50}	TI[c]	MIC_{50}	TI	MIC_{50}	TI	MIC_{50}	TI
GS	—	21.1 (±2.6)	7.9 (±0.8)	2.7 (1.0)	8.0 (±0.0)	2.6 (1.0)	11.0 (±0.4)	1.9 (1.0)	13.1 (±0.0)	1.6 (1.0)
1	Phe	78.7 (±4.2)	15.8 (±0.0)	4.9 (1.8)	23.6 (±0.0)	3.3 (1.3)	24.8 (±1.2)	3.1 (1.7)	>40	nd
2	Dip	34.0 (±3.7)	3.8 (±0.8)	8.9 (3.3)	3.4 (±0.5)	10.0 (3.8)	20.3 (±0.3)	1.7 (0.9)	23.9 (±2.1)	1.4 (0.9)
3	Flg	2.1 (±1.4)	2.2 (±0.1)	0.9 (0.3)	2.2 (±0.2)	0.9 (0.3)	5.0 (±0.3)	0.4 (0.2)	14.3 (±1.9)	0.1 (0.1)
5	Tic	7.7 (±1.5)	2.4 (±0.2)	3.2 (1.2)	2.4 (±0.1)	3.2 (1.2)	5.1 (±0.1)	1.5 (0.8)	8.5 (±2.1)	0.9 (0.6)
6	(*R*,*R*)c$_3$diPhe	26.0 (±2.4)	3.2 (±0.5)	8.1 (3.0)	5.1 (±0.5)	5.1 (1.9)	>40	nd[e]	>40	nd
7	(*S*,*S*)c$_3$diPhe	>60	25.8 (±0.0)	2.3 (0.8)	>30	nd	>40	nd	>40	nd
8	Ac$_3$c	>60	>30	nd	>30	nd	>40	nd	>40	nd
9	(*S*,*S*)c$_3$Phe	>60	>30	nd	>30	nd	>40	nd	>40	nd
10	(*R*,*R*)c$_3$Phe	>60	>30	nd	>30	nd	>40	nd	41.0 (±11)	nd
11	(*S*,*R*)c$_3$Phe	57.0 (±3.8)	>30	nd	>30	nd	>40	nd	>40	nd
12	(*R*,*S*)c$_3$Phe	>60	>30	nd	>30	nd	>40	nd	>40	nd
13	(αMe)Phe	56.5 (±3.9)	11.9 (±1.0)	4.7 (1.7)	6.8 (±0.3)	8.3 (3.2)	9.6 (±0.4)	5.9 (3.1)	7.0 (±1.4)	8.0 (5.0)

[a] HC_{50}: peptide concentration required for 50% lysis of sheep erythrocytes; MIC_{50}: peptide concentration required for 50% inhibition of bacterial growth after 24 h, relative to a control culture; standard deviations for HC_{50} and MIC_{50} are shown in parentheses. [b] Phe*[5,5′] stands for Phe or the corresponding surrogate (see Figures 1 and 2); GS contains D-Phe[4,4′]. [c] TI = therapeutic index = HC_{50}/MIC_{50}; values relative to TI of GS in parentheses. [d] An *A. baumannii* strain resistant to colistin (polymyxin E). [e] nd = not determined.

GS is mostly active against Gram-positives, the last two strains were included in view of the growing incidence of *A. baumannii* infections, particularly those caused by strains resistant to polymyxin E, which until recently has been the last universally active drug against these pathogens.[48] Microbicidal activities were determined in solution, as in solid media they tend to be underestimated, especially for Gram-negatives.[4] *Pseudomonas aeruginosa*, another Gram-negative, was included earlier on in the assays, but as none of the analogues showed growth inhibitions above 30% at 50 μM, the highest concentration assayed, it was disregarded. Results are given in Table 3 and show that the replacement of the D-Phe-Pro sequences in GS by D-Pro-Phe in **1** has a negative impact on activity. However, further modification of the Phe residue allows the recovery and even an enhancement of the microbicidal potency of the natural peptide. Thus, the Dip (**2**), Flg (**3**), Tic (**5**), and (*R*,*R*)c$_3$diPhe (**6**) analogues turned out to be more active than GS against Gram-positive bacteria, while **3** and **5** were also superior against Gram-negatives. The improved microbicidal activity of the Tic analogue (**5**) against the colistin-resistant strain is also worth mentioning. On the other hand, the Ac$_3$c derivative (**8**), lacking an aromatic moiety at the β-turn region, was, perhaps not surprisingly, practically devoid of any antibiotic activity.

The contrasting activity of the analogues incorporating the c$_3$diPhe enantiomers (**6**, **7**) deserves some comment. Thus, while **7** had the lowest activity against all bacterial strains among the **1**−**7** subset, **6** was unique in its highest selectivity for Gram-positives. These differences, which might be ascribed to the rigid orientation imposed by the cyclopropane ring on the aromatic substituents, prompted us to expand the analogue series with the four c$_3$Phe stereoisomers bearing a single phenyl group (Figure 2). Surprisingly enough, all analogues containing these Phe surrogates (**9**−**12**) showed marginal activity, if at all, against all organisms. In contrast, the analogue with the closely related (αMe)Phe residue (**13**) not only retained the activity of GS but displayed the best therapeutic index (TI, see below) against both *A. baumannii* strains.

The hemolytic effect of the peptides was evaluated on sheep erythrocytes as an indicator of toxicity against mammalian cells. Results are summarized in Table 3, where the therapeutic index (TI, defined as HC_{50}/MIC_{50}) is also given as a combined measure of both effects. As a general rule, the antibiotic and hemolytic activities were found to run parallel. Thus, peptides with very low microbicidal power (**1**, **7**−**12**) were hardly harmful to erythrocytes, whereas analogues of high antibiotic activity (**3**, **5**) turned out to be also fairly toxic. However, some notable deviations to this general behavior

were observed. For instance, the Dip analogue **2** was more active against Gram-positives yet slightly less cytotoxic than GS, which translated into a modest (about 3-fold) but significant TI increase vs GS. A similar improvement in TI was observed for the (*R*,*R*)$c_3$diPhe-containing analogue (**6**) regarding the *S. aureus* strain. The peptide incorporating (αMe)Phe (**13**) was found to be essentially harmless to erythrocytes while exhibiting an antibiotic potency similar or even superior to that of GS, which resulted in an enhanced TI for all pathogens considered. Particularly noteworthy is the fact that the most significant increase in TI for this analogue (near 5-fold that of the natural peptide) was observed for the Gram-negative *A. baumannii* strand resistant to conventional antibiotics. It should also be noted that improved TIs reported in the literature for GS analogues most often stem from lower cytotoxicity,[24,25,27,49,50] whereas the most significant increases in TI relative to GS found in this work (≥3-fold) are also associated to a higher antibiotic potency.

Discussion

Several groups, including our own,[25,29−32] have shown that the β-turn of GS is particularly suited to modulation of the TI by subtle substitutions. In this work, we have explored the impact of replacing Phe by residues bearing one or two phenyl rings that impart different degrees of hydrophobicity, bulkiness, and rotational freedom to the GS molecule. To carry out these substitutions with minimal perturbation of the β-turn architecture, the native D-Phe-L-Pro sequence of GS has been changed to D-Pro-L-Phe because it is known that simple residue permutation (i.e., to L-Pro-D-Phe) results in practically full loss of activity.[22] This distinguishing feature of the present series compares favorably with our earlier work,[25] where the canonical D-Phe-L-Pro β-turn was used. In absolute terms, sequence inversion to D-Pro-L-Phe, as exemplified by analogue **1**, entails a certain loss of antimicrobial potency relative to the parent GS. However, the change also involves a substantial decrease in cytotoxicity (determined as hemolysis) that, when factored into the therapeutic index (TI), actually results in an almost 2-fold improvement against the Gram-positive *S. aureus* as well as the colistin-sensitive strain of the Gram-negative *A. baumannii*. A similarly improved antimicrobial profile can be found for the **2** (Dip) and **6** [(*R*,*R*)$c_3$diPhe] analogues against Gram-positives, as well as for the (αMe)Phe replacement (**13**) against both Gram-positives and -negatives. The Tic replacement, which in the previous series proved to be very advantageous,[25] is now (analogue **5**) of less consequence, as the enhanced antimicrobial potency entails a considerable penalty in cytotoxicity. In the canonical D-Phe-L-Pro series,[25] the proximity between Orn and the aromatic side chain exclusive of the Tic analogue was invoked to explain the TI improvement. Such interaction is not observed in **5**, neither in **3**, the most hemolytic analogue (Tables 2−3). Interestingly, however, Orn-Phe* NOEs are observed for analogues less hemolytic than GS, such as **1** and **2** (Tables 2−3).

Among several factors known to influence the interaction of AMPs with bacterial or mammalian membranes, hydrophobicity is viewed as crucial. In general, and regardless of the anionic or zwitterionic nature of the bilayer, a hydrophobic patch of size above a minimal threshold is required for a peptide to partition into the membrane. In this scenario, hydrophobicity correlates relatively well with AMP activity against systems such as eukaryotes (e.g., hemolysis) or Gram-positive bacteria, where the peptide can diffuse relatively easily through the peptidoglycan layer.

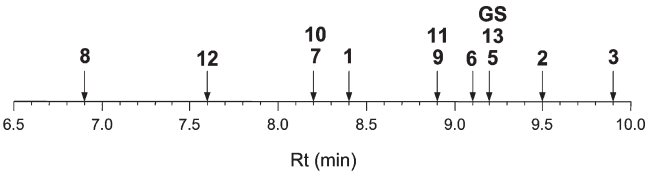

Figure 5. Retention times (R_t) of GS analogues on RP-HPLC. Elution conditions: see Experimental Section. The retention time of GS under the same conditions is also shown for comparison.

For GS and the 12 analogues of the present series, however, hydrophobicity does not provide a straightforward interpretation to antimicrobial action. RP-HPLC retention times (Figure 5), widely accepted as a criterion of relative hydrophobicity for structurally related compounds, clearly show that while the least (**8**) and most (**3**) hydrophobic analogues, respectively, show low and high activities against Gram-positives and erythrocytes, analogues of intermediate hydrophobicity follow no discernible general trend in this regard. For instance, the four c_3Phe derivatives (**9**−**12**) differ significantly in hydrophobicity but coincide in (a very poor) activity. Again, comparing GS with **2** or **5**, of similar hydrophobicity but higher potency against Gram-positives, reveals similar discrepancies, albeit in the opposite sense. The fact that the antimicrobial performance of the current set of analogues cannot be explained simply on the basis of hydrophobicity agrees with recent data on AMPs like lactoferricin[51] or again GS,[52] for which additional parameters (e.g., bulkiness) have been invoked as crucial for activity.

Against Gram-negatives, the situation is more complex due to the existence of an outer membrane that AMPs must traverse before interacting with the plasma membrane. In this context, hydrophobicity can be regarded as a two-edged sword because, above a certain limit, it will induce aggregation and poor water solubility, causing the AMP to be sequestered within the outer membrane, unable to reach and disrupt the plasma membrane. Thus, a balanced combination of hydrophobicity with additional parameters such as amphipathicity, molecular flexibility, or cationic character becomes essential for AMP interaction with the LPS of the outer membrane and efficacy against Gram-negatives. In the present work, improved performance against Gram-negatives is observed for analogues **3**, **5**, and **13**, all of them with hydrophobicities (i.e., retention times) equal or superior to GS and with substantial structural diversity as Phe surrogates (i.e., Flg in **3**, Tic in **5**, (αMe)Phe in **13**). The failure of analogues **6**−**12** against Gram-negatives may be explained because, in these analogues, the bulkiness and rigidity of the cyclopropane system may dramatically impair AMP transit through the membrane, regardless of its potential to disrupt the plasma membrane final target.

Changes in antimicrobial activity patterns were evident not only between Gram-positive and Gram-negative organisms but also at the species or even the strain level. The case of the Gram-negative pathogen *Acinetobacter baumannii*, of which both colistin-susceptible and -resistant strains that reflect differences in outer membrane composition were tested, is illustrative. Against this organism, a substantially improved TI was found for analogue **13** (3-fold relative to the parent GS for the colistin-sensitive strain), making this peptide an optimized lead within the current D-Pro-L-Phe series, with the added incentive that the TI optimization applies also to the

resistant strain, which constitutes a serious clinical concern[53] given that colistin is the last drug universally active on this pathogen. It has been proposed that the self-uptake mechanism used by GS to traverse the outer membrane of Gram-negatives differs from the more general one of other membrane-active AMPs,[54] for which high-affinity binding to LPS (mediated by both hydrophobicity and cationic character) entails disruption of the outer membrane and access to the periplasmic space. For GS, instead, the mechanism would involve diffuse binding to LPS and further passage driven by hydrophobic interactions. This alternative mechanism would not seem to apply to the current set of analogues, because the resistant strain, with a highly modified LPS, is significantly more insensitive to analogues such as **3** or **5**, which incorporate Phe* surrogates equally or more hydrophobic than Phe. Also, recent experiments have shown the permeability of the outer membrane to be quite compromised in the resistant strain.[55]

In summary, although inversion of the β-turn sequence of GS has a detrimental impact on antibiotic potency, this can be productively offset by the incorporation of Phe surrogates containing an additional aromatic group or a single phenyl substituent with the adequate orientation. Because the NMR data, with the probable exception of analogues **2** and **12** (see Results), do not reveal substantial alterations in conformation, it is fair to assume that, as long as a robust global β-sheet structure is preserved, sequence inversion at the β-turn of GS is a productive source of antimicrobial leads, provided that a modicum of hydrophobicity is preserved and that the conformational restriction involved is not inadequate (as in the cyclopropane analogues except **6**). As is often the case in SAR studies of peptides, subtle changes such as the addition of a methyl group (compare analogues **1** and **13**) can have a dramatic impact on the biological profile. Thus, as shown by analogues **7** and **9**−**12**, structural constraints imposing inadequate orientation of the aromatic substituent at the β-turn of GS can be highly detrimental for antibiotic potency. In contrast, analogues **2**, **6**, and **13** show a remarkable 3-fold boost in TI against Gram-positives relative to GS. Of these, **6** is selective for Gram-positives and, more interestingly, analogue **13** is quite effective against Gram-negatives, including an interesting 5-fold increase in TI against the colistin-resistant *Acinetobacter* strain.

Experimental Section

Chemicals and Instrumentation for Peptide Synthesis. The different stereoisomers of $c_3$diPhe,[38] c_3Phe,[39] and fluorenylglycine[40] were prepared as previously reported. Dibenzylglycine was obtained following the methodology described by Kotha.[41] *N*-Boc ornithine was purchased from Bachem (Bubendorf, Switzerland), and its side-chain amino group was protected as a formamide by reaction with formic acid and 1,1′-oxalyldiimidazole.[42] All other amino acids were purchased from Senn Chemicals (Dielsdorf, Switzerland), NeoMPS (Strasbourg, France), or Fluka (Buchs, Switzerland). Chloromethylated Merrifield resin and TFMSA were from Fluka, HATU from GenScript (Piscataway, NJ), and HBTU from Matrix Innovation (Montreal, Quebec). Solvents and other chemicals were from SDS (Peypin, France). Mass determination was done by the ESI technique in a MicrOTOF-Q spectrometer (Bruker Daltonics, Billerica, MA). Analytical RP-HPLC was performed on an LC-2010A workstation (Shimadzu Corporation, Kyoto, Japan) with a Luna C_8 (3 μm, 50 mm × 4.6 mm) column (Phenomenex BV, Utrecht, The Netherlands) eluted with a linear 5−95% gradient of CH_3CN (+0.036% TFA, v/v) into H_2O (+0.045% TFA, v/v) over 15 min at 1 mL/min flow rate, with UV detection at 220 nm. Preparative RP-HPLC purification was done on a Phenomenex Luna C_8 column (10 μm, 250 mm × 10 mm) running linear gradients of CH_3CN (+0.1% TFA, v/v) into H_2O (+0.1% TFA, v/v) as indicated for each peptide, at a flow rate of 5 mL/min. The preparative system included two Shimadzu LC-8A pumps, a Shimadzu SPD-10A detector and a Foxy Jr. fraction collector (Teledyne Isco, Lincoln, NE).

General Procedure for Peptide Synthesis. All peptides were synthesized manually by solid-phase methods on a Boc-D-Pro-Merrifield resin (0.1 mmol) using Boc chemistry. Boc-amino acids (0.3 mmol) were coupled by HBTU/DIEA (0.3 and 0.6 mmol, respectively) for 30−45 min in DMF. HATU was used instead of HBTU for the coupling reactions involving the 5/5′ residues. To avoid diketopiperazine formation, the third amino acid of each sequence was incorporated by the *in situ* neutralization method.[56] Coupling and deprotection reactions were monitored by the nynhidrin[57] or *p*-nitrophenylester[58] colorimetric tests. The linear decapeptide was cleaved from the resin by treatment with TFA/TFMSA/TIS 10:1:1 (v/v/v) (4 mL) at room temperature for 90 min and then precipitated with cold *tert*-butyl methyl ether. The peptide was redissolved in glacial acetic acid, filtered off the resin, and lyophilized. Cyclization was performed by dissolving the peptide in DMF to a final concentration of 2 mg/mL and stirring for 1 h at room temperature in the presence of HATU/HOAt/DIEA (3:3:5 equiv). After solvent removal and lyophilization, the cyclized peptide was deformylated by treatment with 20% hydrochloric acid in methanol at 37 °C for 21 h. The solvent was evaporated under reduced pressure, and the residue was taken up in glacial acetic acid and lyophilized. Final purification was carried out by preparative reversed-phase HPLC as indicated in each case. HPLC-homogeneous fractions were combined and lyophilized to give white powders of ≥99% HPLC purity (see Supporting Information). Variations to this general protocol are indicated for each peptide.

***cyclo*(Val-Orn-Leu-D-Pro-Phe)$_2$ (1).** RP-HPLC, linear 30−70% CH_3CN gradient into H_2O for 30 min (66 mg, 0.063 mmol, 47% overall yield). HRMS (ESI) $C_{60}H_{93}N_{12}O_{10}$ $[M + H]^+$: calcd 1141.7132, found 1141.7088; $C_{60}H_{92}N_{12}O_{10}Na$ $[M + Na]^+$: calcd 1163.6952, found 1163.6924.

***cyclo*(Val-Orn-Leu-D-Pro-Dip)$_2$ (2).** RP-HPLC, linear 45−75% CH_3CN gradient into H_2O for 30 min (55 mg, 0.042 mmol, 34% overall yield). HRMS (ESI) $C_{72}H_{101}N_{12}O_{10}$ $[M + H]^+$: calcd 1293.7758, found 1293.7682; $C_{72}H_{100}N_{12}O_{10}Na$ $[M + Na]^+$: calcd 1315.7578, found 1315.7521.

***cyclo*(Val-Orn-Leu-D-Pro-Flg)$_2$ (3).** RP-HPLC, linear 35−65% CH_3CN gradient into H_2O for 30 min (57 mg, 0.044 mmol, 38% overall yield). HRMS (ESI) $C_{72}H_{97}N_{12}O_{10}$ $[M + H]^+$: calcd 1289.7445, found 1289.7420; $C_{72}H_{96}N_{12}O_{10}Na$ $[M + Na]^+$: calcd 1311.7265, found 1311.7228.

***cyclo*(Val-Orn-Leu-D-Pro-Tic)$_2$ (5).** The cyclized peptide was purified by RP-HPLC (linear 60−90% CH_3CN gradient into H_2O for 30 min) prior to deformylation. Final RP-HPLC, linear 40−70% CH_3CN gradient into H_2O for 30 min (52 mg, 0.045 mmol, 39% overall yield). HRMS (ESI) $C_{62}H_{93}N_{12}O_{10}$ $[M + H]^+$: calcd 1165.7132, found 1165.7088; $C_{62}H_{92}N_{12}O_{10}Na$ $[M + Na]^+$: calcd 1187.6952, found 1187.6895.

***cyclo*[Val-Orn-Leu-D-Pro-(*R*,*R*)$c_3$diPhe]$_2$ (6).** Precipitation of the linear decapeptide by addition of cold *tert*-butyl methyl ether proved unsuccessful. The organic solvent was then evaporated and the crude was redissolved in CH_3CN. The peptide precipitated upon addition of H_2O. The cyclization mixture was allowed to react overnight. The cyclized peptide was purified by RP-HPLC (linear 65−95% CH_3CN gradient into H_2O for 30 min) prior to deformylation. Final RP-HPLC, linear 40−75% CH_3CN gradient into H_2O for 30 min (24 mg, 0.018 mmol, 15% overall yield). HRMS (ESI) $C_{74}H_{101}N_{12}O_{10}$ $[M + H]^+$: calcd 1317.7758, found 1317.7737; $C_{74}H_{100}N_{12}O_{10}Na$ $[M + Na]^+$: calcd 1339.7578, found 1339.7557.

***cyclo*[Val-Orn-Leu-D-Pro-(*S*,*S*)$c_3$diPhe]$_2$ (7).** The linear decapeptide was precipitated with H_2O, as described above for **6**. Final RP-HPLC, linear 40−75% CH_3CN gradient into H_2O for 30 min (64 mg, 0.049 mmol, 41% overall yield). HRMS (ESI) $C_{74}H_{101}N_{12}O_{10}$ $[M + H]^+$: calcd 1317.7758, found 1317.7717; $C_{74}H_{100}N_{12}O_{10}Na$ $[M + Na]^+$: calcd 1339.7578, found 1339.7559.

***cyclo*(Val-Orn-Leu-D-Pro-Ac_3c)$_2$ (8).** RP-HPLC, linear 30−60% CH_3CN gradient into H_2O for 30 min (68 mg, 0.067 mmol, 59% overall yield). HRMS (ESI) $C_{50}H_{85}N_{12}O_{10}$ $[M + H]^+$: calcd. 1013.6506, found 1013.6494; $C_{50}H_{84}N_{12}O_{10}Na$ $[M + Na]^+$: calcd 1035.6326, found 1035.6309.

***cyclo*[Val-Orn-Leu-D-Pro-(*S*,*S*)c_3Phe]$_2$ (9).** The linear decapeptide was precipitated with H_2O, as described above for **6** and purified by RP-HPLC (linear 40−70% CH_3CN gradient into H_2O for 30 min) before cyclization. The cyclized peptide was purified by RP-HPLC (linear 50−80% CH_3CN gradient into H_2O for 30 min) prior to deformylation. Final RP-HPLC, linear 40−70% CH_3CN gradient into H_2O for 30 min (61 mg, 0.052 mmol, 45% overall yield). HRMS (ESI) $C_{62}H_{93}N_{12}O_{10}$ $[M + H]^+$: calcd 1165.7132, found 1165.7088; $C_{62}H_{92}N_{12}O_{10}Na$ $[M + Na]^+$: calcd 1187.6952, found 1187.6912.

***cyclo*[Val-Orn-Leu-D-Pro-(*R*,*R*)c_3Phe]$_2$ (10).** The linear decapeptide was precipitated with H_2O, as described above for **6**, and purified by RP-HPLC (linear 45−75% CH_3CN gradient into H_2O for 30 min) before cyclization. The cyclized peptide was purified by RP-HPLC (linear 50−80% CH_3CN gradient into H_2O for 30 min) prior to deformylation. Final RP-HPLC, linear 35−65% CH_3CN gradient into H_2O for 30 min (49 mg, 0.042 mmol, 36% overall yield). HRMS (ESI) $C_{62}H_{93}N_{12}O_{10}$ $[M + H]^+$: calcd 1165.7132, found 1165.7102; $C_{62}H_{92}N_{12}O_{10}Na$ $[M + Na]^+$: calcd 1187.6952, found 1187.6928.

***cyclo*[Val-Orn-Leu-D-Pro-(*S*,*R*)c_3Phe]$_2$ (11).** RP-HPLC, linear 45−65% CH_3CN gradient into H_2O for 30 min (26 mg, 0.021 mmol, 18% overall yield). HRMS (ESI) $C_{62}H_{93}N_{12}O_{10}$ $[M + H]^+$: calcd 1165.7132, found 1165.7117; $C_{62}H_{92}N_{12}O_{10}Na$ $[M + Na]^+$: calcd 1187.6952, found 1187.6947.

***cyclo*[Val-Orn-Leu-D-Pro-(*R*,*S*)c_3Phe]$_2$ (12).** The cyclization step required an additional amount of the HATU/HOAt/DIEA (0.6:0.6:1.0 equiv) coupling mixture. RP-HPLC, linear 35−60% CH_3CN gradient into H_2O for 30 min (67 mg, 0.057 mmol, 50% overall yield). HRMS (ESI) $C_{62}H_{93}N_{12}O_{10}$ $[M + H]^+$: calcd 1165.7132, found 1165.7116; $C_{62}H_{92}N_{12}O_{10}Na$ $[M+Na]^+$: calcd 1187.6952, found 1187.6939.

***cyclo*[Val-Orn-Leu-D-Pro-(αMe)Phe]$_2$ (13).** RP-HPLC, linear 35−65% CH_3CN gradient into H_2O for 30 min (76 mg, 0.065 mmol, 56% overall yield). HRMS (ESI) $C_{62}H_{97}N_{12}O_{10}$ $[M + H]^+$: calcd 1169.7445, found 1169.7458; $C_{62}H_{96}N_{12}O_{10}Na$ $[M + Na]^+$: calcd 1191.7265, found 1191.7261.

NMR Spectroscopy. Samples for NMR experiments were prepared at 1−2 mM peptide concentration in 0.5 mL of H_2O/D_2O 9:1 (v/v) or pure D_2O at pH 3.0. pH was measured with a glass microelectrode and was not corrected for isotope effects. NMR spectra were acquired on a Bruker AV 600 MHz spectrometer equipped with a *z*-gradient cryoprobe. A methanol sample was used to calibrate the temperature of the NMR probe. One-dimensional (1D) and two-dimensional (2D) spectra were acquired by standard pulse sequences using presaturation of the water signal. Mixing times for 2D TOCSY and NOESY were 60 and 150 ms, respectively. The $^1H-^{13}C$ and $^1H-^{15}N$ HSQC spectra[59] at natural ^{13}C and ^{15}N abundance were recorded in D_2O and H_2O/D_2O 9:1 (v/v), respectively. Data were processed using TOPSPIN (Bruker Biospin, Rheinstetten, Germany) software. Sodium 2,2-dimethyl-2-silapentane-5-sulfonate (DSS) was used as an internal reference for ^1H chemical shifts. The ^{13}C and ^{15}N chemical shifts were indirectly calibrated by multiplying the spectrometer frequency that corresponds to 0 ppm in the ^1H spectrum, assigned to internal DSS reference, by 0.25144954 and 0.101329118, respectively.[60] The ^1H NMR signals of the peptides were assigned by sequential assignment methods.[61] The ^{13}C and ^{15}N resonances were then assigned following the cross-correlations observed in the HSQC spectra between the proton and the heteronucleus to which it is bonded.

Structure Calculation. Structure calculations were performed by using the CYANA program[62] and an annealing strategy. Because the nonproteinogenic amino acids were not included in the standard CYANA libraries, we built them using MOLMOL[63] and manual optimization (these libraries are available upon request from the authors). For this purpose, X-ray data of compounds containing these amino acids were obtained from our laboratories or retrieved from the Cambridge Structural Database.[64] Theoretical constraints for the GS β-sheet incorporated for structure calculation included ϕ and ψ angle restraints, lower and upper-limit distance restraints for the four characteristic cross-strand hydrogen-bonds, and upper-limit distance restraints for the backbone atoms of strand residues (see Supporting Information). Experimental distance constraints for peptides **1** and **5** were derived from 2D NOESY spectra recorded in H_2O/D_2O 9:1 (v/v). The NOE cross-peaks were integrated by using the automatic integration subroutine of the Sparky program (T. D. Goddard and S. G. Kneller, University of California at San Francisco) and then calibrated and converted to upper-limit distance constraints with CYANA.[62] Given the symmetrical nature of the peptides, for structure calculations, residues were renumbered from 1 to 10 starting at Leu3 (Figure 1). Lower and upper limit restraints required for peptide backbone cyclization were introduced with CYANA (see Supporting Information). For each peptide, a total of 50 conformers were generated and the 20 conformers with the lowest target function were analyzed. Model structures were examined with MOLMOL.[63] A side chain torsion angle was considered as well-defined when its root-mean-square deviation between values in the 20 best calculated structures was less than ±30°.

Antimicrobial Activity. Stocks of *Staphylococcus aureus* CECT 240, *Listeria monocytogenes* CECT 4032, *Acinetobacter baumannii* ATCC 19606, and its isogenic colistin-resistant strain 19606R (obtained by continuous growing under increasing colistin concentration) were maintained at −80 °C in freezing medium (65% glycerol, 0.1 M $MgSO_4$, 25 mM Tris-HCl, pH 8.0). Two days prior to the assay for microbicidal activity, they were thawed and grown in MBH medium (Mueller-Hinton II Broth Cation Adjusted (Becton-Dickinson, Cockeysville, MD)) at 37 °C; for 19606R, 64 μg/mL colistin sulfate (Sigma, Madrid, Spain) was included.[47] Bacterial cells were harvested at exponential growth phase, washed twice with phosphate buffered saline (PBS, 10 mM Na_2HPO_4, 1 mM KH_2PO_4, 140 mM NaCl, 3 mM KCl, pH 7.0), and resuspended in MBH, at 5×10^5 colony forming units/mL. Aliquots (100 μL) from this suspension were transferred into a polypropylene 96-well plate, and bacteria were allowed to proliferate for 24 h at 37 °C in the presence of the corresponding peptide concentration. Afterward, growth was measured by turbidimetry at 600 nm in a model 680 microplate reader (Bio-Rad Laboratories, Hercules. CA). Determinations were carried out twice on triplicated samples. MIC_{50} was defined as the lowest peptide concentration inhibiting bacterial growth by 50%, relative to untreated control, and was calculated using the SigmaPlot (Systat Software, San Jose, CA) software, v. 9.0.

Hemolytic Activity Assay. As above, hemolytic activity of the peptides was also determined twice on triplicate samples. Defibrinated sheep blood (Biomedics, Madrid, Spain) was centrifuged and washed twice with Hank's medium (136 mM NaCl, 4.2 mM Na_2HPO_4, 4.4 mM KH_2PO_4, 5.4 mM KCl, 4.1 mM $NaHCO_3$, pH 7.2), supplemented with 20 mM D-glucose (Hank's-Glc). Erythrocytes were resuspended in the same buffer at 2×10^7 erythrocytes/mL, and 100 μL aliquots of the suspension were incubated with the peptides (4 h, 37 °C). The remaining erythrocytes were harvested in a Micro 200 microfuge (A. Hettich GmbH & Co. KG, Germany) (14000 rpm, 5 min, 4 °C), 80 μL of the supernatant were transferred into a 96-well culture microplate,

and released hemoglobin was determined at 550 nm in a Bio Rad 680 (Hercules, CA) microplate reader. The asymptotic ordinate of the GS supernatant was taken as 100% hemolysis. HC_{50} values were calculated using SigmaPlot, version 9.0.

Acknowledgment. This work was supported by Ministerio de Ciencia e Innovación (BIO2008-04487-CO3-02 to D.A., CTQ2008-00080/BQU to M.A.J., CTQ2007-62245 to C.C.), Fondo de Investigaciones Sanitarias (PI061125, PS09/1928, and RD06/0021/0006 to L.R.), by the regional governments of Aragón (research group E40), Catalonia (SGR2008-492), and Madrid (COMBACT S-BIO-0260/2006). C.S. and C.M.S. thank Ministerio de Educación y Ciencia and Consejo Superior de Investigaciones Científicas-European Social Fund for FPU and I3P fellowships, respectively. This project has been funded in whole or in part with federal funds from the National Cancer Institute, National Institutes of Health, under contract number HHSN261200800001E. The content of this publication does not necessarily reflect the view of the policies of the Department of Health and Human Services, nor does mention of trade names, commercial products, or organization imply endorsement by the U.S. Government. This research was supported (in part) by the Intramural Research Program of the NIH, National Cancer Institute, Center for Cancer Research.

Supporting Information Available: NMR data, details on structure calculations, and analytical data on the peptides synthesized. This material is available free of charge via the Internet at http://pubs.acs.org.

References

(1) Hirsch, T.; Jacobsen, F.; Steinau, H. U.; Steinstraesser, L. Host defense peptides and the new line of defence against multiresistant infections. *Protein Pept. Lett.* **2008**, *15*, 238–243.
(2) Parisien, A.; Allain, B.; Zhang, J.; Mandeville, R.; Lan, C. Q. Novel alternatives to antibiotics: bacteriophages, bacterial cell wall hydrolases, and antimicrobial peptides. *J. Appl. Microbiol.* **2008**, *104*, 1–13.
(3) Gause, G. F. Gramicidin S and its use in the treatment of infected wounds. *Nature* **1944**, *154*, 703.
(4) Kondejewski, L. H.; Farmer, S. W.; Wishart, D. S.; Hancock, R. E.; Hodges, R. S. Gramicidin S is active against both Gram-positive and Gram-negative bacteria. *Int. J. Pept. Protein. Res.* **1996**, *47*, 460–466.
(5) Prenner, E. J.; Lewis, R. N.; McElhaney, R. N. The interaction of the antimicrobial peptide gramicidin S with lipid bilayer model and biological membranes. *Biochim. Biophys. Acta* **1999**, *1462*, 201–221.
(6) Hull, S. E.; Karlsson, R.; Main, P.; Woolfson, M. M.; Dodson, E. J. The crystal structure of a hydrated gramicidin S-urea complex. *Nature* **1978**, *275*, 206–207.
(7) Schmidt, G. M.; Hodgkin, D. C.; Oughton, B. M. A crystallographic study of some derivatives of gramicidin S. *Biochem. J.* **1957**, *65*, 744–750.
(8) Tishchenko, G. N.; Andrianov, V. I.; Vainstein, B. K.; Woolfson, M. M.; Dodson, E. Channels in the gramicidin S-with-urea structure and their possible relation to transmembrane ion transport. *Acta Crystallogr., Sect. D: Biol. Crystallogr.* **1997**, *53*, 151–159.
(9) Ovchinnikov, Y. A.; Ivanov, V. T. Conformational states and biological activity of cyclic peptides. *Tetrahedron* **1975**, *31*, 2177–2209.
(10) Jelokhani-Niaraki, M.; Hodges, R. S.; Meissner, J. E.; Hassenstein, U. E.; Wheaton, L. Interaction of gramicidin S and its aromatic amino-acid analogs with phospholipid membranes. *Biophys. J.* **2008**, *95*, 3306–3321.
(11) Katsu, T.; Kobayashi, H.; Fujita, Y. Mode of action of gramicidin S on *Escherichia coli* membrane. *Biochim. Biophys. Acta* **1986**, *860*, 608–619.
(12) Afonin, S.; Glaser, R. W.; Berditchevskaia, M.; Wadhwani, P.; Guhrs, K. H.; Mollmann, U.; Perner, A.; Ulrich, A. S. 4-fluorophenylglycine as a label for ^{19}F NMR structure analysis of membrane-associated peptides. *ChemBioChem* **2003**, *4*, 1151–1163.
(13) Arai, T.; Imachi, T.; Kato, T.; Ogawa, H. I.; Fujimoto, T.; Nishino, N. Synthesis of [hexafluorovalyl$^{1,1'}$]gramicidin S. *Bull. Chem. Soc. Jpn.* **1996**, *69*, 1383–1389.
(14) Waki, M.; Abe, O.; Okawa, R.; Kato, T.; Makisumi, S.; Izumiya, N. Studies of peptide antibiotics. XII. Syntheses of [2,2′-α,γ-diaminobutyric acid]-and [2,2′-lysine]-gramicidin S. *Bull. Chem. Soc. Jpn.* **1967**, *40*, 2904–2909.
(15) Aimoto, S. The synthesis of a heavy-atom derivative of gramicidin S (GS), [D-Phe(4-Br)$^{4,4'}$]-GS, by a novel method. *Bull. Chem. Soc. Jpn.* **1988**, *61*, 2220–2222.
(16) Andreu, D.; Ruiz, S.; Carreño, C.; Alsina, J.; Albericio, F.; Jiménez, M. A.; de la Figuera, N.; Herranz, R.; García-López, M. T.; González-Muñiz, R. IBTM-containing gramicidin S analogs: evidence for IBTM as a suitable type II′ β-turn mimetic. *J. Am. Chem. Soc.* **1997**, *119*, 10579–10586.
(17) Grotenbreg, G. M.; Buizert, A. E.; Llamas-Saiz, A. L.; Spalburg, E.; van Hooft, P. A.; de Neeling, A. J.; Noort, D.; van Raaij, M. J.; van der Marel, G. A.; Overkleeft, H. S.; Overhand, M. β-Turn modified gramicidin S analogs containing arylated sugar amino acids display antimicrobial and hemolytic activity comparable to the natural product. *J. Am. Chem. Soc.* **2006**, *128*, 7559–7565.
(18) Kawai, M.; Yamamura, H.; Tanaka, R.; Umemoto, H.; Ohmizo, C.; Higuchi, S.; Katsu, T. Proline residue-modified polycationic analogs of gramicidin S with high antibacterial activity against both Gram-positive and Gram-negative bacteria and low hemolytic activity. *J. Pept. Res.* **2005**, *65*, 98–104.
(19) Lee, D. L.; Hodges, R. S. Structure−activity relationships of de novo designed cyclic antimicrobial peptides based on gramicidin S. *Biopolymers* **2003**, *71*, 28–48.
(20) Ripka, W. C.; Delucca, G. V.; Bach, A. C.; Pottorf, R. S.; Blaney, J. M. Protein β-turn mimetics II: Design, synthesis and evaluation in the cyclic peptide gramicidin S. *Tetrahedron* **1993**, *49*, 3609–3628.
(21) Sato, K.; Kato, R.; Nagai, U. Studies on β-turn of peptides. XII. Synthetic conformation of weak activity of [D-Pro$^{5,5'}$]-Gramicidin S predicted from β-turn preference of its partial sequence. *Bull. Chem. Soc. Jpn.* **1986**, *59*, 535–538.
(22) Tamaki, M.; Okitsu, T.; Araki, M.; Sakamoto, H.; Takimoto, M.; Muramatsu, I. Synthesis and properties of gramicidin S analogs containing Pro-D-Phe sequence in place of D-Phe-Pro sequence in the β-turn part of the antibiotic. *Bull. Chem. Soc. Jpn.* **1985**, *58*, 531–535.
(23) Wishart, D. S.; Kondejewski, L. H.; Semchuk, P. D.; Sykes, B. D.; Hodges, R. S. A method for the facile solid-phase synthesis of gramicidin S and its analogs. *Lett. Pept. Sci.* **1996**, *3*, 53–60.
(24) Yamada, K.; Shinoda, S. S.; Oku, H.; Komagoe, K.; Katsu, T.; Katakai, R. Synthesis of low-hemolytic antimicrobial dehydropeptides based on gramicidin S. *J. Med. Chem.* **2006**, *49*, 7592–7595.
(25) Solanas, C.; de la Torre, B. G.; Fernández-Reyes, M.; Santiveri, C. M.; Jiménez, M. A.; Rivas, L.; Jiménez, A. I.; Andreu, D.; Cativiela, C. Therapeutic index of gramicidin S is strongly modulated by D-phenylalanine analogs at the β-turn. *J. Med. Chem.* **2009**, *52*, 664–674.
(26) Jelokhani-Niaraki, M.; Kondejewski, L. H.; Farmer, S. W.; Hancock, R. E.; Kay, C. M.; Hodges, R. S. Diastereoisomeric analogs of gramicidin S: structure, biological activity and interaction with lipid bilayers. *Biochem. J.* **2000**, *349*, 747–755.
(27) Kondejewski, L. H.; Jelokhani-Niaraki, M.; Farmer, S. W.; Lix, B.; Kay, C. M.; Sykes, B. D.; Hancock, R. E.; Hodges, R. S. Dissociation of antimicrobial and hemolytic activities in cyclic peptide diastereomers by systematic alterations in amphipathicity. *J. Biol. Chem.* **1999**, *274*, 13181–13192.
(28) Abraham, T.; Marwaha, S.; Kobewka, D. M.; Lewis, R. N.; Prenner, E. J.; Hodges, R. S.; McElhaney, R. N. The relationship between the binding to and permeabilization of phospholipid bilayer membranes by GS14dK4, a designed analog of the antimicrobial peptide gramicidin S. *Biochim. Biophys. Acta* **2007**, *1768*, 2089–2098.
(29) Kawai, M.; Nagai, U. Comparison of conformation and antimicrobial activity of synthetic analogs of gramicidin S: stereochemical considerations of the role of D-phenylalanine in the antibiotic. *Biopolymers* **1978**, *17*, 1549–1565.
(30) Higashijima, T.; Miyazawa, T.; Kawai, M.; Nagai, U. Gramicidin S analogs with a D-Ala, Gly, or L-Ala residue in place of the D-Phe residue: molecular conformations and interactions with phospholipid membrane. *Biopolymers* **1986**, *25*, 2295–2307.
(31) Ando, S.; Aoyagi, H.; Waki, M.; Kato, T.; Izumiya, N. Studies of peptide antibiotics. XLIII. Syntheses of gramicidin S analogs containing D-serine or dehydroalanine in place of D-phenylalanine and asymmetric hydrogenation of the dehydroalanine residue. *Tetrahedron Lett.* **1982**, *23*, 2195–2198.
(32) Grotenbreg, G. M.; Spalburg, E.; de Neeling, A. J.; van der Marel, G. A.; Overkleeft, H. S.; van Boom, J. H.; Overhand, M. Synthesis

and biological evaluation of novel turn-modified gramicidin S analogs. *Bioorg. Med. Chem.* **2003**, *11*, 2835–2841.
(33) Rose, G. D.; Gierasch, L. M.; Smith, J. A. Turns in peptides and proteins. *Adv. Protein Chem.* **1985**, *37*, 1–109.
(34) Marraud, M.; Aubry, A. Crystal structures of peptides and modified peptides. *Biopolymers* (*Pept. Sci.*) **1996**, *40*, 45–83.
(35) Hutchinson, E. G.; Thornton, J. M. A revised set of potentials for beta-turn formation in proteins. *Protein Sci.* **1994**, *3*, 2207–2216.
(36) Jiménez, A. I.; Cativiela, C.; Aubry, A.; Marraud, M. β-Turn preferences induced by 2,3-methanophenylalanine chirality. *J. Am. Chem. Soc.* **1998**, *120*, 9452–9459.
(37) Toniolo, C.; Crisma, M.; Formaggio, F.; Peggion, C. Control of peptide conformation by the Thorpe−Ingold effect (Cα-tetrasubstitution). *Biopolymers* (*Pept. Sci.*) **2001**, *60*, 396–419.
(38) Jiménez, A. I.; López, P.; Oliveros, L.; Cativiela, C. Facile synthesis and highly efficient resolution of a constrained cyclopropane analog of phenylalanine. *Tetrahedron* **2001**, *57*, 6019–6026.
(39) Cativiela, C.; Díaz-de-Villegas, M. D.; Jiménez, A. I.; López, P.; Marraud, M.; Oliveros, L. Efficient access to all four stereoisomers of phenylalanine cyclopropane analogs by chiral HPLC. *Chirality* **1999**, *11*, 583–590.
(40) Royo, S.; Jiménez, A. I.; Cativiela, C. Synthesis of enantiomerically pure β,β-diphenylalanine (Dip) and fluorenylglycine (Flg). *Tetrahedron: Asymmetry* **2006**, *17*, 2393–2400.
(41) Kotha, S.; Behera, M. Synthesis and modification of dibenzylglycine derivatives via the Suzuki−Miyaura coupling reaction. *J. Pept. Res.* **2004**, *64*, 72–85.
(42) Kitagawa, T.; Arita, J.; Nogahata, A. Convenient one-pot method for formylation of amines and alcohols using formic acid and 1,1′-oxalyldiimidazole. *Chem. Pharm. Bull.* (*Tokyo*) **1994**, *42*, 1655–1657.
(43) Wishart, D. S.; Bigam, C. G.; Holm, A.; Hodges, R. S.; Sykes, B. D. ^{1}H, ^{13}C and ^{15}N random coil NMR chemical shifts of the common amino acids. I. Investigations of the nearest-neighbor effects. *J. Biomol. NMR* **1995**, *5*, 67–81.
(44) Schubert, M.; Labudde, D.; Oschkinat, H.; Schmieder, P. A software tool for the prediction of Xaa-Pro peptide bond conformations in proteins based on ^{13}C chemical shift statistics. *J. Biomol. NMR* **2002**, *24*, 149–154.
(45) Santiveri, C. M.; Rico, M.; Jiménez, M. A. $^{13}C_{\alpha}$ and $^{13}C_{\beta}$ chemical shifts as a tool to delineate β-hairpin structures in peptides. *J. Biomol. NMR* **2001**, *19*, 331–345.
(46) Wishart, D. S.; Sykes, B. D.; Richards, F. M. Relationship between nuclear magnetic resonance chemical shift and protein secondary structure. *J. Mol. Biol.* **1991**, *222*, 311–333.
(47) Santiveri, C. M.; Rico, M.; Jiménez, M. A. Position effect of cross-strand side-chain interactions on beta-hairpin formation. *Protein Sci.* **2000**, *9*, 2151–2160.
(48) Saugar, J. M.; Rodríguez-Hernández, M. J.; de la Torre, B. G.; Pachón-Ibáñez, M. E.; Fernández-Reyes, M.; Andreu, D.; Pachón, J.; Rivas, L. Activity of cecropin A-melittin hybrid peptides against colistin-resistant clinical strains of *Acinetobacter baumannii*: molecular basis for the differential mechanisms of action. *Antimicrob. Agents Chemother.* **2006**, *50*, 1251–1256.
(49) Kondejewski, L. H.; Lee, D. L.; Jelokhani-Niaraki, M.; Farmer, S. W.; Hancock, R. E. W.; Hodges, R. S. Optimization of microbial specificity in cyclic peptides by modulation of hydrophobicity within a defined structural framework. *J. Biomol. Chem.* **2002**, *1*, 67–74.
(50) McInnes, C.; Kondejewski, L. H.; Hodges, R. S.; Sykes, B. D. Development of the structural basis for antimicrobial and hemolytic activities of peptides based on gramicidin S and design of novel analogs using NMR spectroscopy. *J. Biol. Chem.* **2000**, *275*, 14287–14294.
(51) Haug, B. E.; Strøm, M. B.; Svendsen, J. S. The medicinal chemistry of short lactoferricin-based antibacterial peptides. *Curr. Med. Chem.* **2007**, *14*, 1–18.
(52) Van der Knaap, M.; Engels, E.; Busscher, H. J.; Otero, J. M.; Llamas-Saiz, A. L.; van Raaij, M. J.; Mars-Groenendijk, R. H.; Noort, D.; van der Marel, G. A.; Overkleeft, H. S.; Overhand, M. Synthesis and biological evaluation of asymmetric gramicidin S analogues containing modified D-phenylalanine residues. *Bioorg. Med. Chem.* **2009**, *17*, 6318–6328.
(53) Valencia, R.; Arroyo, L. A.; Conde, M.; Aldana, J. M.; Torres, M. J.; Fernández-Cuenca, F.; Garnacho-Montero, J.; Cisneros, J. M.; Ortiz, C.; Pachón, J.; Aznar, J. Nosocomial outbreak of infection with pan-drug-resistant *Acinetobacter baumannii* in a tertiary care university hospital. *Infect. Control Hosp. Epidemiol.* **2009**, *30*, 257–263.
(54) Zhang, L.; Dhillon, P.; Yan, H.; Farmer, S.; Hancock, R. E. Interactions of bacterial cationic peptide antibiotics with outer and cytoplasmic membranes of *Pseudomonas aeruginosa*. *Antimicrob. Agents Chemother.* **2000**, *44*, 3317–3321.
(55) Fernández-Reyes, M.; Rodríguez-Falcón, M.; Chiva, C.; Pachón, J.; Andreu, D.; Rivas, L. The cost of resistance to colistin in *Acinetobacter baumannii*: a proteomic perspective. *Proteomics* **2009**, *9*, 1632–1645.
(56) Schnölzer, M.; Alewood, P.; Jones, A.; Alewood, D.; Kent, S. B. In situ neutralization in Boc-chemistry solid phase peptide synthesis. Rapid, high yield assembly of difficult sequences. *Int. J. Pept. Protein Res.* **1992**, *40*, 180–193.
(57) Kaiser, E.; Colescott, R. L.; Bossinger, C. D.; Cook, P. I. Color test for detection of free terminal amino groups in solid-phase synthesis of peptides. *Anal. Biochem.* **1970**, *34*, 595–598.
(58) Madder, A.; Farcy, N.; Hosten, N. G. C.; De Muynck, H.; De Clercq, P. J.; Barry, J.; Davies, A. P. A novel sensitive colorimetric assay for visual detection of solid phase bound amines. *Eur. J. Org. Chem.* **1999**, 2787–2791.
(59) Bax, A.; Lerner, L. Two-dimensional nuclear magnetic resonance spectroscopy. *Science* **1986**, *232*, 960–967.
(60) Markley, J. L.; Bax, A.; Arata, Y.; Hilbers, C. W.; Kaptein, R.; Sykes, B. D.; Wright, P. E.; Wüthrich, K. Recommendations for the presentation of NMR structures of proteins and nucleic acids—IUPAC-IUBMB-IUPAB Inter-Union Task Group on the standardization of data bases of protein and nucleic acid structures determined by NMR spectroscopy. *J. Biomol. NMR* **1998**, *12*, 1–23.
(61) Wüthrich, K.; Billeter, M.; Braun, W. Polypeptide secondary structure determination by nuclear magnetic resonance observation of short proton-proton distances. *J. Mol. Biol.* **1984**, *180*, 715–740.
(62) Güntert, P. Automated NMR structure calculation with CYANA. *Methods Mol. Biol.* **2004**, *278*, 353–378.
(63) Koradi, R.; Billeter, M.; Wüthrich, K. MOLMOL: a program for display and analysis of macromolecular structures. *J. Mol. Graphics* **1996**, *14* (51−55), 29–32.
(64) Allen, F. H. The Cambridge Structural Database: a quarter of a million crystal structures and rising. *Acta Crystallogr., Sect. B: Struct. Sci.* **2002**, *58*, 380–388.